REAL-TIME SYSTEM IDENTIFICATION OF AIRCRAFT DYNAMICS USING TIME-FREQUENCY WAVELET ANALYSIS

Masaru Naruoka, Takuma Hino, Takeshi Tsuchiya
The University of Tokyo

Keywords: *System identification, Robustness, Wavelet, Time-frequency, UAV*

Abstract

In this paper, a new analytical method for system identification is proposed. This method is intended for real-time monitoring of the flight characteristic of aircraft and especially considers robustness against the flight condition compared to other existing methods. This method is characterized by the use of time-frequency information, which is provided by wavelet transform. The time-frequency information is used to cut off noisy data in terms of both time and frequency. The performance of the proposed method is validated by applying it to two targets: simulated mass-spring-damper system, and a small uninhabited aerial vehicle (UAV). The results show that the proposed method works well even in difficult conditions, and performs sufficiently accurate identification.

1 Introduction

This study is motivated by the newly emerging demands for real-time acquisition of mathematical models of aircraft dynamics. For example, for civil aircraft, continuous monitoring of its dynamics during flight can be used to detect any abnormalities. In addition, real-time modeling using such data can help online reconstruction or adaptation of control modules to safely make emergency landings when sudden defects occur.

This new demand is quite different from conventional demands, which are mainly intended for acquisition of time-invariant characteristics. In other words, although the conventional demands are met by offline methods such as wind tunnel tests, the new one requires online methods with thoroughly short time delays.

Thus, this study utilizes system identification techniques. The system identification is based on a simple idea; if input values and observable variables of a target system are measured, and the system is sufficiently excited by carefully designed input, the system can be estimated by analyzing the measured data. This indicates that the system identification can be easily applied to the online acquisition of the flight characteristic, because it only requires flight log such as time histories of angle of attack and deflection of control surfaces.

In fact, system identification has been used to acquire the flight characteristic, and improved as a verification methodology of the wind tunnel tests. This implies that the accuracy of the estimated parameters, which depends on not only analytical methods but also the measured data obtained by the flight tests, is mainly focused in the conventional applications. In other words, arrangement of the flight tests such as selecting flight area where the wind is stable is as, or more essential than performing appropriate analysis in order to obtain better results.

Comparing with requirements for the conventional system identification techniques and this study, the most significant difference is that the system identification of this study must work well even under severe environment such as strong gust. Therefore, the conventional application of the system identification is insufficient for the purpose of this study in terms of the ro-

bustness against the flight condition. Although there are Fourier transform regression (FTR) [2] and unscented Kalman filter (UKF) [4], both of which have such robustness by using band-pass frequency filter and considering nonlinearity, respectively, these methods are not theoretically free from deterioration by the strong disturbance and require complicated tuning based on the noise characteristic in order to perform good estimation.

Therefore, we propose a new analytical method of the system identification named wavelet filtered regression (WFR). WFR utilizes wavelet transform to provide time-frequency information, which makes easier to extract meaningful information content from the noisy flight log. While Fourier transform, which is the fundamental algorithm of FTR, also gives such feature by repeatedly applying to short period data, wavelet transform is superior to Fourier transform. This is because wavelet transform automatically balances the trade-off between the accuracy and calculation delay of the information. In addition, a filtering mechanism is introduced. This mechanism is based on some reasonable assumptions, for example, if the input is preferably strong, the system is sufficiently excited against the disturbance and easily identified. It works with the time-frequency information, which clarifies the signal strength in the aspects of time and frequency, and theoretically enhances the robustness against the noise. The detail of this new method is explained in Sect. 2.

To validate the performance of WFR, an example problem, which estimates parameters of a simple mass-spring-damper model, is firstly studied. Its detail and results are elaborated in Sect. 3, and comparisons with other methods are also shown. Then, system identification of the longitudinal stability derivatives of a small UAV is demonstrated in Sect. 4. Small UAVs are defined as fixed wing type aircraft and their wingspan and weight are about one meter and one kilogram, respectively. The reason why the small UAV is chosen is that the flight log of these UAVs are far noisier than larger aircraft mainly because they are disturbed by gust easily, and still is a challenge to estimate its flight dynamics.

In this paper, the flight tests of the small UAV is also explained in Sect. 4. This is because experiments employing such small UAVs are a new field and there are many problems. The most critical problem is the strict limitations small UAVs have on size and weight of their payload. These limitations make it impossible to use accurate sensors, which are essential to obtain accurate flight data. In order to solve this problem, we developed new special avionics, which consists of a small INS/GPS navigation unit and air data sensor.

2 Wavelet Filtered Regression (WFR) as Proposed Method

In this section, WFR, the proposed method, which is characterized by using Wavelet transform and the filtering mechanism, is explained. Firstly, in addition to wavelet transform, multi-resolution analysis, which is an effective way to calculate time-frequency information, is described briefly. Then, the filtering mechanism called parallel-projection using multi-resolution analysis (PPMRA), which enhances the robustness against noise, is introduced. Finally, WFR, which integrates PPMRA and recursive least square (RLS), is explained.

2.1 Wavelet Transform and Multi-resolution Analysis

Wavelet transform converts time series data $f(t)$ into time-frequency information $\mathfrak{W}(a,b)$ by

$$\mathfrak{W}(a,b) \equiv \int_{-\infty}^{+\infty} f(t) \frac{1}{\sqrt{a}} \psi^* \left(\frac{t-b}{a} \right) dt, \quad (1)$$

where a, b are scaling and shift parameter which correspond to frequency and time, respectively, and ψ^* is a mother wavelet function. Compared to Fourier transform, which converts time series data $f(t)$ into frequency series $\mathfrak{F}(\omega)$ with focusing on a corresponding angular speed ω like:

$$\mathfrak{F}(\omega) \equiv \int_{-\infty}^{+\infty} f(t) e^{i\omega t} dt, \quad (2)$$

wavelet transform has two arguments, a and b. This characterizes wavelet transform as a good way to handle time-series data whose frequency changes temporally. For example, a signal f_{chirp} and its power spectra calculated by both wavelet and Fourier transforms are shown in Fig. 1, whose middle, top, and bottom subfigures correspond to these items. The signal f_{chirp} is a chirp signal whose frequency moves higher as time passes like

$$f_{\text{chirp}}(t) = \sin\left(\frac{\pi}{900}t^2\right), \tag{3}$$

and the strongest part of its true power spectrum should also be shifted to higher frequency as time passes. Although the power spectrum calculated by Fourier transform cannot express the change, power spectra calculated by wavelet transform describes it clearly.

In reality, measured data such as flight log is not continuous time series data, and is discretized by certain sampling time. To apply such type of data, discrete wavelet transform (DWT) is utilized. Furthermore, time-frequency information can be calculated effectively by choosing parameters a, b and mother wavelet function ψ^* appropriately. The calculation procedure is shown in Fig. 2, which depicts that by cascading higher time-frequency information calculated by a transform to another transform, lower time-frequency information is determined. This is multi-resolution analysis (MRA), and is utilized in this study. It is also noted that Daubechies wavelet [1] is used as its mother wavelet.

2.2 PPMRA: Parallel Projection using Multi-Resolution Analysis

In this subsection, the idea and procedure of PPMRA, the filtering mechanism, is elaborated.

Typically, a postulated model, which defines parameters to be estimated in the system identification scheme, is linear and summarized as

$$\frac{d\underline{x}}{dt} = A\underline{x} + \underline{u} + \underline{v}, \tag{4}$$

when $\underline{x}$, $\underline{u}$, and A are state variables, input values, and a coefficient matrix, respectively. $\underline{v}$ is process noise, which cannot be measured.

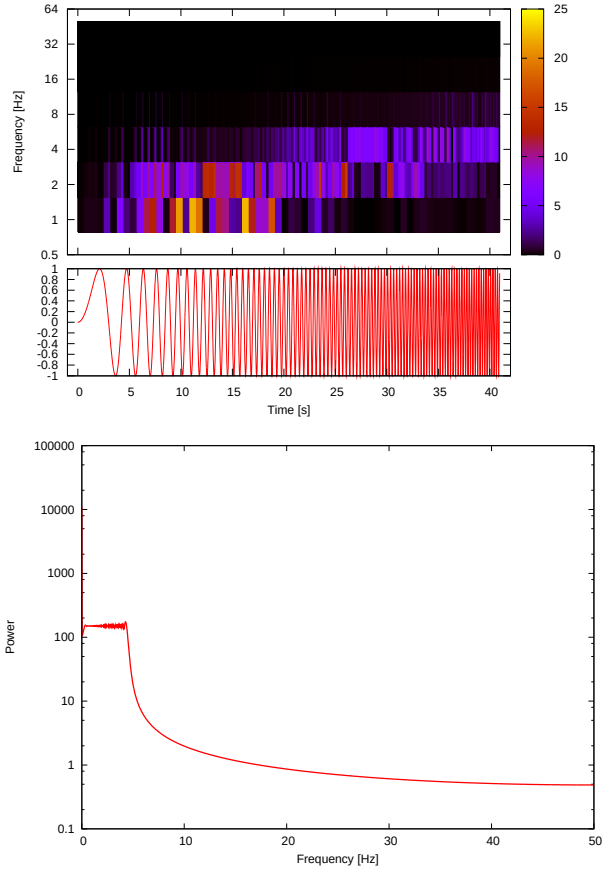

Fig. 1 Chip signal (middle) and its power spectra calculated by wavelet (top) and Fourier (bottom) transform. The power spectrum calculated by wavelet transform, whose power strength is shown by color, depicts clearly the change of frequency as time passes.

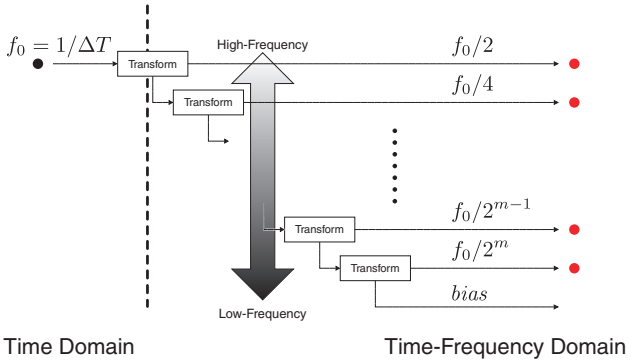

Fig. 2 Procedure of multi-resolution analysis (MRA), which convert periodically-sampled data represented by a black point to time-frequency information represented by red points.

Here, the input values $\underline{u}$ is assumed to be represented by summation of oscillation like

$$\underline{u} = \sum \underline{f} e^{\omega t}. \tag{5}$$

Then, by neglecting process noise $\underline{v}$, state variables $\underline{x}$ of Eq. (4) can be solved analytically as

$$\underline{x} = \left(\sum_i C_i \underline{x}_{0,i} e^{\lambda_{0,i} t} \right) + \sum (\omega I - A)^{-1} \underline{f} e^{\omega t}, \tag{6}$$

where the first term of the right-hand side is called as the general solution, which consists of another coefficient matrix C_i, eigen values $\lambda_{0,i}$ and eigen vectors $\underline{x}_{0,i}$ of matrix A. The second term is also called as the special solution, which correlates with the input values $\underline{u}$, because it contains the same elements $\underline{f}$ and $e^{\omega t}$ of $\underline{u}$.

If the system is nearly stable, that is, the trim $\underline{x}_0$ is nearly constant, the second term is dominant and the first term is negligible. This implies that, when the input values $\underline{u}$ change periodically in some frequency in addition to such stability, the state variables $\underline{x}$ also change periodically in the same frequency. Therefore, by only focusing on frequencies in which the input values include, we can extract desirable relation of the state variables and input values and estimate the coefficient matrix A more accurately. This is the idea of PPMRA.

PPMRA is approved under some assumptions as described above, and their validity will be discussed below. The first is that process noise $\underline{v}$ is neglected. This is reasonable, because when the system is controllable, the input excites the system sufficiently against the process noise. Moreover, the assumption can be easily achieved when the input and noise differ in terms of frequency, because PPMRA only focuses on the portion of the system which correlates to the input frequency. The second is about the stability of the system. Any system can be considered as stable in a pretty short time, which is enough to apply MRA in order to extract periodically changes by using time-frequency information. Thus, the second assumption is reasonable to consider the system as nearly stable when MRA is utilized. In addition, most aircraft can fly stable without controlling actively. The third assumption is that the input values changes periodically, which is validated in this study because they can be controlled arbitrary. Furthermore, the input is usually designed to include broad frequency band by using combination of pulse pattern represented by the 3-2-1-1 and M-series random inputs [3]. The last is that there is no difficulty to focus on certain frequency. Using MRA solves this problem, because unlike Fourier transform, MRA can extract time-frequency information even though the periodically changes are instantaneous.

The procedure of PPMRA will be explained by using an example shown in Fig. 3. Firstly, the state variables and the input values are converted from time-series data to time-frequency information by MRA. This first process is shown in the subfigures on the first and second rows of Fig. 3. In the figure, the angle of attack α and elevator deflection δ_e represent the state variables and input values, respectively. Then, the time-frequency information of the state variables $\mathfrak{W}_{\text{state}}$ is suppressed if the strength of the corresponding time-frequency information $\mathfrak{W}_{\text{input}}$ is lower than a threshold Δ. The second process is depicted by using an operator $\otimes$ on the second row of the figure, and its applied results is shown in the subfigure on the third row. The operator $\otimes$ is exactly written in the form of an equation as

$$\begin{aligned} &\mathfrak{W}_{\text{left}}(a,b) \otimes \mathfrak{W}_{\text{right}}(a,b) \\ &\quad \equiv \begin{cases} \textit{if } a \neq 0 \\ \quad \textit{and } \mathfrak{W}_{\text{right}}(a,b) \geq \Delta \textit{ then} \\ \quad \mathfrak{W}_{\text{left}}(a,b) \\ \textit{else} \\ \quad 0 \end{cases}. \end{aligned} \tag{7}$$

The reason why the suppression is always occurred at $a = 0$ is to eliminate the bias, which is unnecessary for the analysis. These two processes explained above are the procedure of PPMRA.

The subfigure on the forth row of the Fig. 3 is shown in order to indicate the effectiveness of PPMRA. It is the reconstructed time-series data of angle of attack and calculated from the results

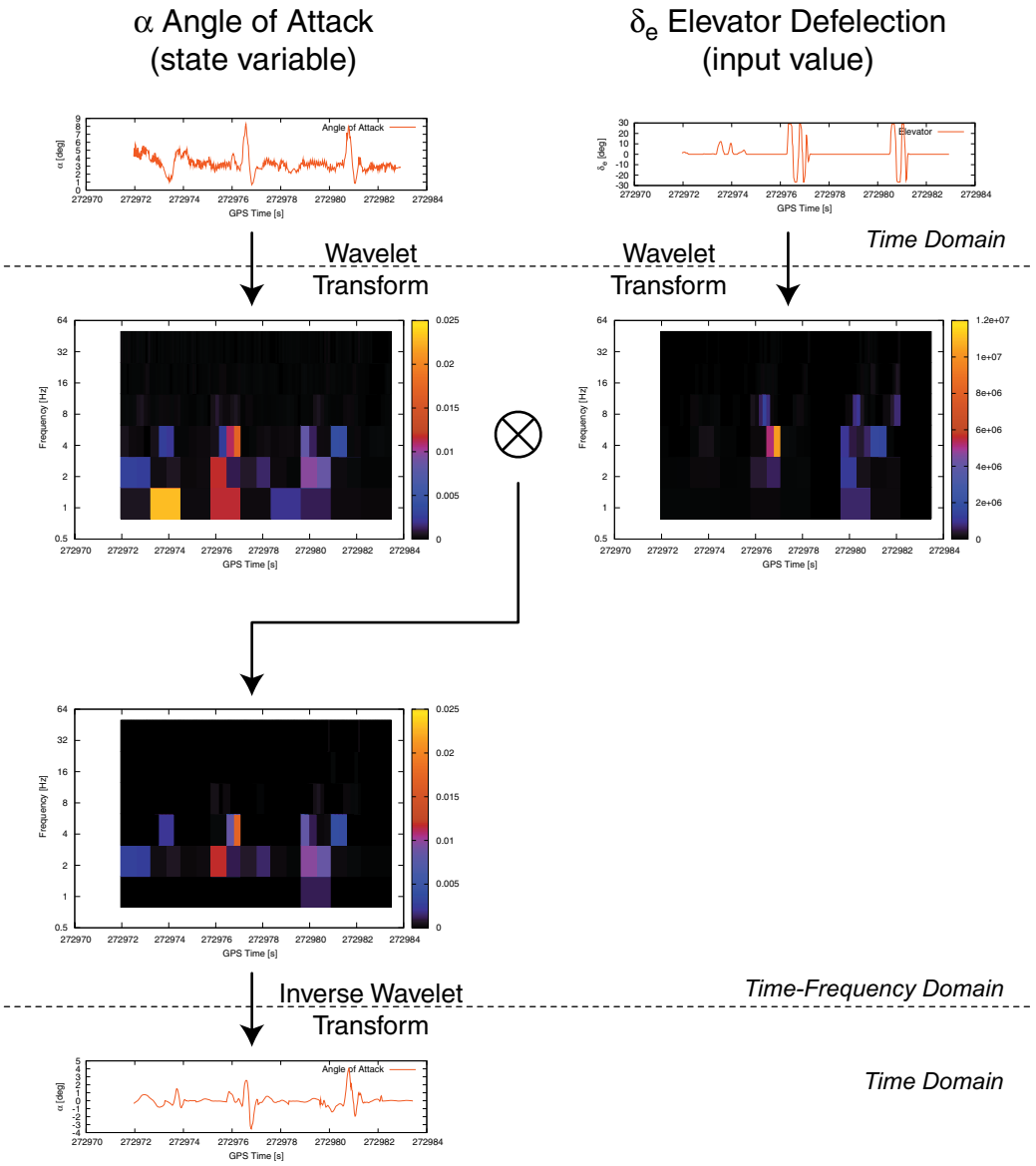

Fig. 3 Example results of PPMRA. The angle of attack is filtered by the elevator deflection input with PPMRA. The bottom subfigure shows the PPMRA results as the time-series data, which are purposely calculated by inverse wavelet transform and redundant description.

of PPMRA on the third row by inverse wavelet transform. Compared the subfigure on the forth row to the left one on the first row, the change localized around GPS time 272973s is recognized as process noise and suppressed because there is no input around this time. In addition, small vibration which exists in entire time is also removed as the measurement noise because its frequency does not correspond to one of the input. These features provided by PPMRA are useful for the system identification.

It is noted that PPMRA named after the idea of subspace identification [5, 7], which is a general approach to system identification of a complex system. In the subspace identification, by applying orthogonal transform such as singular value decomposition (SVD), a target identified system will be separated into deterministic and stochastic subsystems. Here, to determine parameters of a postulated model equals to analyze the deterministic subsystem, which is called as the parallel projection part of the system. Therefore, the proposed filtering method can been seen as analyzing the parallel projection parts ex-

tracted by MRA.

2.3 Wavelet Filtered Regression (WFR)

WFR is the proposed system identification method, which combines PPMRA and RLS like shown in Fig. 4.

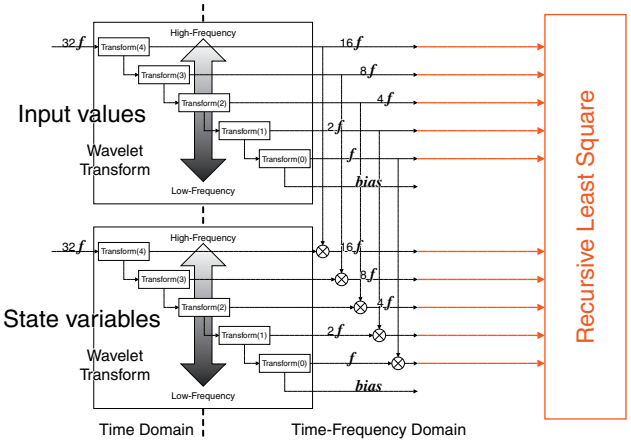

Fig. 4 Wavelet filtered regression (WFR)

RLS is the well-known simplest system identification method, but does not have robustness against process noise. To compensate for the weakness of RLS, PPMRA is utilized as the filtering process before application of RLS. Although the data filtered by PPMRA can be reconstructed in time series data with inverse wavelet transform, the input data of RLS is the time-frequency series data, that is, the direct outputs of PPMRA, to reduce the calculation cost. The reason why the direct outputs can be used as the input of RLS is easily understood by applying wavelet transform to both sides of Eq. (4) as

$$\mathfrak{W}_{\frac{d\underline{x}}{dt}}(a,b) = A\mathfrak{W}_{\underline{x}}(a,b) + \mathfrak{W}_{\underline{u}}(a,b), \quad (8)$$

where capital $\mathfrak{W}$ represents a wavelet transformed value of a subscript value. Here, the coefficient matrix A, which is supposed to be estimated by RLS, is or can be seen as constant and invariant under the transform. Therefore, the time-frequency information directly given by PPMRA can be used as the input of RLS. WFR can continuously estimate parameters with preferably short delay and is categorized as an online method, because both PPMRA and RLS have capability to process data sample by sample.

3 Example Parameter Estimation of Mass-spring-damper Model using WFR

This section describes the example problem in order to evaluate the performance of WFR. Computational simulations is utilized to generate required data, because it can exactly control the difficulties of the problem. In the following subsections, the model postulation, simulation conditions and results are explained.

3.1 Postulated Models and Simulation Conditions

The target system of the problem is a simple mass-spring-damper model represented as

$$\frac{d}{dt}\begin{pmatrix}\dot{x}\\ x\end{pmatrix} = \begin{bmatrix}-0.5 & -3\\ 1 & 0\end{bmatrix}\begin{pmatrix}\dot{x}\\ x\end{pmatrix} + \begin{pmatrix}u+v\\ 0\end{pmatrix}, \quad (9)$$

where $x, \dot{x}$ are the position and velocity, respectively, and compose state variables. u is the controllable input, and corresponds to the force. v is process noise pertaining to the input. Parameters to be estimated are the coefficient matrix of the first term of the right hand side, that is, $-0.5, -3, 1$ and 0 are the solutions of this problem. The eigen modes of this system are calculated by performing eigenvalue decomposition to the coefficient matrix. They are damped oscillation and indicated by one conjugate pair of complex values. The natural frequency of the system indicated by these eigen modes is about $100\mathrm{deg}/\mathrm{s}$ in angular speed.

To make the problem realistic, it is assumed that all the state variables cannot be obtained directly. The observable variables are defined as the following observation equation:

$$\tilde{x} = \begin{bmatrix}0 & 1\end{bmatrix}\begin{pmatrix}\dot{x}\\ x\end{pmatrix} + w, \quad (10)$$

which indicates that only the position $\tilde{x}$ is explicitly observable, but deteriorated by measurement noise w. This also implies that if the velocity $\dot{x}$ is

required for the estimation, it must be calculated with numerical differential of the position x.

The evaluations are conducted under combinations of the following conditions.

- RLS, FTR and WFR are utilized as the estimation methods.
- The waveform of the input u is sinusoidal or chirp signal. The angular speed of the sinusoidal wave is $50, 100$ or 200 deg/s. The angular speed of the chirp signal changes gradually from 0 to 200deg/s. The magnitude of the input is adjusted to excite the system sufficiently.
- The process noise v is either zero or a white noise. The white noise influences the input u, and its magnitude is 5 deg/s in phase error.
- The measurement noise w is a white noise, and its magnitude is small (0.01) or large (1) in standard deviation.
- The velocity, which cannot be observed directly, is calculated by the first order numerical differential, and there is no mechanism such as low-pass filtering to suppress the numerical noise.
- The frequency band used for FTR ranges from 0.2 to 5 Hz. PPMRA of WFR monitors frequency over 0.2 Hz.
- The calculation step is 0.1 s, that is, the Nyquist frequency is 5 Hz. The length of the analyzed data is 100 s.
- The initial values of the estimated parameters are $\begin{bmatrix} -2 & -1 \\ 0.5 & 0 \end{bmatrix}$ corresponding to the coefficient matrix of Eq. (9).

The results of these estimation are shown by eigen values projected on complex plane. This is because it is difficult to evaluate them by comparing numerical differences between the estimated and true parameters. On the other hand, the closeness of the estimated eigen values to their references can be easily evaluated. Needless to say, the closer the estimated values are to their references, the better it is. It is also noted that the time histories of the estimations are shown in the results, because every method performs the estimation sample by sample.

3.2 Results

Figure 5 shows the estimation results of RLS, FTR and WFR under the easiest condition, that is, the 100 deg/s sinusoidal input, no process noise, and small measurement noise. The reason why the 100 deg/s sinusoidal input is the easiest is because its frequency corresponds to the natural frequency of the system and it excites the system most effectively. Under the easiest condition, FTR and WFR perform the best estimation, and the results of RLS, which seems to be most affected by noise of the numerical differential, are also acceptable. This implies that if the target is under such preferable condition, it is easily identified regardless of the analytical methods.

Figure 6 shows the results under little more difficult condition: the chirp input, no process noise, and small measurement noise. While FTR and WFR still show the same performance as under the easiest condition, the results of RLS change. This indicates that the performance of RLS clearly depends on the nature of the input.

Finally, Fig. 7 shows the results under the most difficult condition, which consists of the chirp input, process noise, and large measurement noise. RLS and FTR completely fail to estimate the true eigen modes, because the fact that the system has natural oscillation is not found. Meanwhile, the results of WFR is relatively acceptable. Therefore, it can be concluded that WFR is superior to RLS and FTR in terms of the robustness against the conditions.

4 Application to small UAV

WFR is also applied to the system identification of the flight characteristic of the small UAV. Small UAVs are easily disturbed by wind and their flight characteristic is difficult to be identified. Therefore, it is suitable to check the performance of WFR with the small UAV. The parameters to be estimated are the dimensional stability derivatives of its longitudinal motion. In the

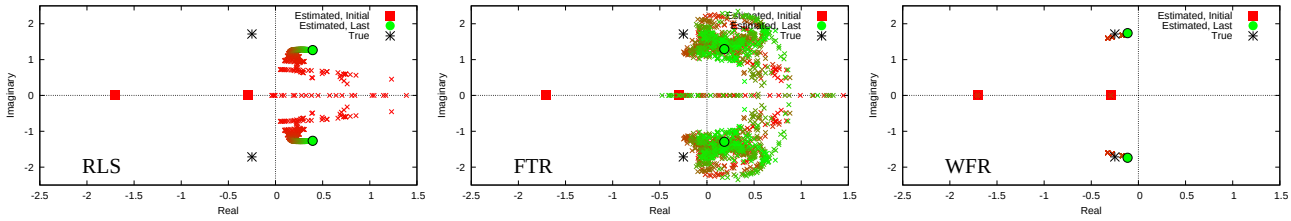

Fig. 5 Estimated eigen modes under the easiest condition

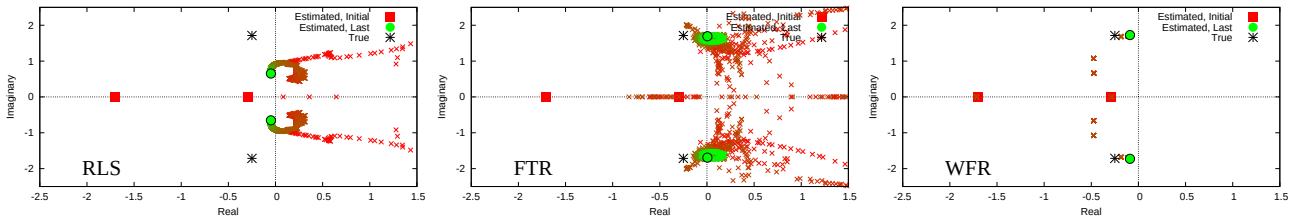

Fig. 6 Estimated eigen modes under the easiest condition except for using the chip input

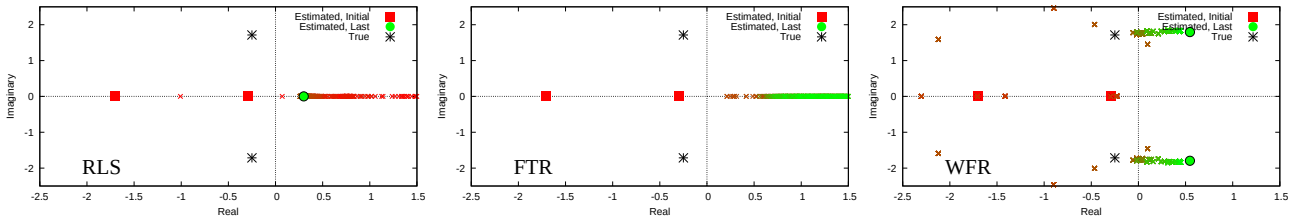

Fig. 7 Estimated eigen modes under the most difficult condition

following subsections, the target UAV, postulated model defining these parameters, data measurement environment required for the identification, and results are elaborated.

4.1 Target small UAV

Figure 8 and Table 1 show a picture and specification of the target small UAV, respectively. Its wingspan and weight is 1.38 m and 2.5kg, which fall within the definition of small UAVs described in the introduction.

Fig. 8 Target small UAV

Table 1 Target small UAV main specifications

Item		Symbol	Value
Main wing	Span [m]	b	1.38
	Area [m^2]	S	0.271
	Aspect ratio	$\mathcal{AR}$	5.32
Overall length [m]		l	1.39
Typical cruise speed [m/s]		U_0	25
Gross weight [kg]		m	2.5
Wing loading [kg/m^2]			9.23

4.2 Postulated model composed of longitudinal stability derivatives

The model is same as one of conventional fixed-wing aircraft and postulated as

$$\frac{d}{dt}\begin{bmatrix} u \\ \alpha \\ q \\ \theta \end{bmatrix} = \begin{bmatrix} X_u & X_\alpha & -W_0 & -g\cos\theta_0 \\ \frac{Z_u}{U_0} & \frac{Z_\alpha}{U_0} & \frac{U_0+Z_q}{U_0} & -\frac{g\sin\theta_0}{U_0} \\ M_u & M_\alpha & M_q & 0 \\ 0 & 0 & 1 & 0 \end{bmatrix}\begin{bmatrix} u \\ \alpha \\ q \\ \theta \end{bmatrix} + \begin{bmatrix} 0 \\ \frac{Z_{\delta_e}}{U_0} \\ M_{\delta_e} \\ 0 \end{bmatrix}\delta_e + \underline{\nu}, \tag{11}$$

where X, Z, M are parameters to be identified and known as the dimensional longitudinal stability derivatives. State variables are perturbation speed u, angle of attack α, pitch rate q, and pitch θ. Symbols with subscript 0 are trim values, and $\underline{v}$ is process noise. Input value is elevator deflection represented as δ_e. It is noted that although derivatives and input related to throttle deflection should be included, these values are omitted in this study because the throttle is difficult to measure and treated as constant.

The state variables are explicitly or implicitly observable defined by the following observation equation:

$$\begin{bmatrix} \tilde{V}_{\text{wind}} \\ \tilde{\alpha} \\ \tilde{q} \\ \tilde{\theta} \end{bmatrix} = \begin{bmatrix} \sqrt{(U_0+u)^2+(W_0+U_0\alpha)^2} \\ \alpha \\ q \\ \theta_0+\theta \end{bmatrix} + \underline{w}, \quad (12)$$

where the left hand side is measured values and $\underline{w}$ is measurement noise.

4.3 Measurement environment

The elevator input δ_e of Eq. (11) and the observable values defined in Eq. (12) are measured in real flight of the small UAV. That required data is measured by the specially developed avionics [6]. This is because existing avionics used in general aircraft is too big and heavy to be installed in the small UAV.

A picture of the developed avionics is shown in Fig. 9. It consists of MEMS INS/GPS navigation unit, air data sensor, and command logger. The navigation unit provides position, velocity and attitude by integrating an inertial navigation system (INS) composed by MEMS sensors, and a global positioning system (GPS) receiver. The air data sensor provides wind speed, angle of attack and side slip angle information accurately and simultaneously using a pitot tube with 5 small orifices. The command logger records the input. This system is very small and light, yet provides sufficiently accurate data for the system identification.

It is noted that in the flight tests, specially designed commands such as 3-2-1-1and doublet are issued to the control surfaces to excite the system effectively after the trim condition has be obtained. Furthermore, wind condition is carefully selected not to affect the flight severely when the tests are carried out.

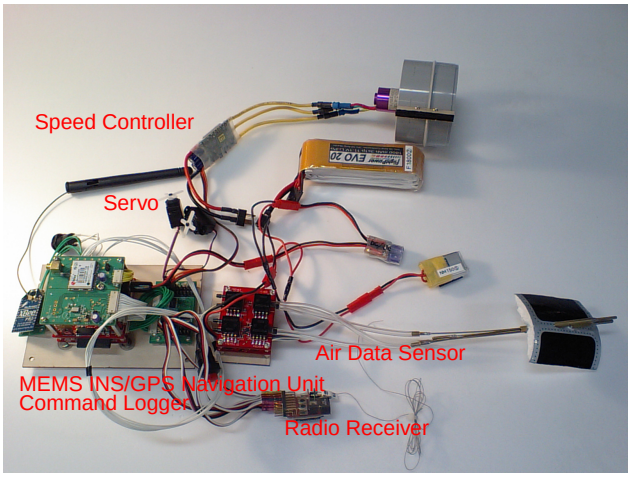

Fig. 9 Image of internal components of the small UAV including the developed avionics

4.4 Results

The estimated parameters of WFR are shown in Table 2 comparing to those of UKF. Reference values of the target parameters, which are obtained by the wind tunnel tests, are also shown in the table. It is difficult to discuss the performance of the results by directly comparing numerical differences of the parameters. Therefore, same as the previous section, the eigen modes shown in Fig. 10 are calculated in order to be discussed. The calculated eigen modes of both WFR and UKF are sufficiently close to the reference those, and it indicates that WFR has the same accuracy of UKF. Considered the fact that UKF has many tuning parameters to keep its performance, it concludes that WFR is comprehensively superior to UKF. It is also noted that the results estimated with RLS and FTR are omitted because their estimation are far worse than those of WFR and UKF.

5 Conclusion

In this study, wavelet filtered regression (WFR), the new analytical method for the system iden-

Table 2 Estimated and reference stability derivatives

Item	Scaling	Ref.	UKF	WFR
X_u	$\times 10^{-2}$	-7.34	63.0	-2.50
X_α	$\times 10^{0}$	5.19	-13.0	2.09
Z_u	$\times 10^{-1}$	-8.91	77.3	1.34
Z_α	$\times 10^{2}$	-1.74	-1.43	-0.25
Z_q	$\times 10^{-1}$	-6.70	33.0	-14.0
Z_{δ_e}	$\times 10^{1}$	-1.69	4.57	-0.36
M_u	$\times 10^{0}$	0	3.50	0.84
M_α	$\times 10^{2}$	-1.07	-0.65	-0.25
M_q	$\times 10^{0}$	-4.63	-5.85	-8.40
M_{δ_e}	$\times 10^{2}$	-1.19	-0.64	-0.72

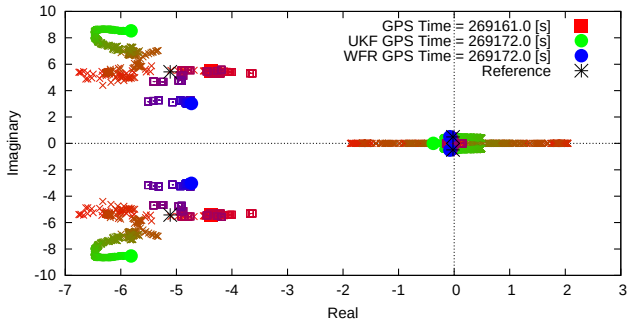

Fig. 10 Eigen modes calculated from results of WFR and UKF

tification was proposed. WFR is characterized by using wavelet transform, which enables the analysis to avoid undesired content via the time-frequency information. This results in the robustness against the conditions under which the required data of the system identification is obtained. The validity of WFR was demonstrated in the two applications. One was the simulated mass-spring-damper system, and showed that WFR was superior to RLS and FTR in terms of both the accuracy and robustness. The other was the small UAV, and also indicated that WFR was as accurate as UKF, which has to be tuned in order to obtain better results. Finally, it concluded that WFR is suitable for the real-time system identification of aircraft dynamics.

Acknowledgment

This study was financially supported by KAKENHI, Grant-in-Aid for JSPS Fellows (21 · 9072).

Contact Author Email Address

fenrir.naru@gmail.com

Copyright Statement

References

[1] Daubechies I. *Ten lectures on wavelets*. Society for Industrial and Applied Mathematics, Philadelphia, PA, USA, 1992.

[2] Eugene. A. M. Real-time parameter estimation in the frequency domain. Technical report, 1999. NASA-aiaa-99-4043.

[3] Jategaonkar R. V. *Flight Vehicle System Identification: A Time Domain Methodology (Progress in Astronautics and Aeronautics)*. AIAA, 2006.

[4] Julier S. J and Uhlmann J. K. A new extension of the kalman filter to nonlinear systems. *Proc Int. Symp. Aerospace/Defense Sensing, Simul. and Controls, Orlando, FL*, pp 182–193, 1997.

[5] Katayama T. *System Identification – Approach by using subspace identification – (in Japanese)*. Asakura Publishing, 2004.

[6] Naruoka M, Hino T, Nakagawa R, Tuchiya T, and Suzuki S. System identification of small uavs with mems-based avionics. *Proc AIAA Infotech@Aerospace 2009 Conference and Exhibit, Seattle, USA*, Apr 2009. AIAA 2009-1907.

[7] Picci G and Katayama T. Stochastic realization with exogenous inputs and "subspace-methods" identification. *Signal Process.*, Vol. 52, No 2, pp 145–160, 1996.